Proceedings of the North American Power Symposium (NAPS), MIT, November 1996, pp.559-565.

Bifurcation Analysis of Induction Motor Loads for Voltage Collapse Studies

Claudio A. Cañizares William Rosehart
University of Waterloo
Department of Electrical & Computer Engineering
Waterloo, ON, Canada N2L 3G1

Abstract—**This paper presents the bifurcation analysis of an aggregated induction motor load with under-load tap-changer transformer and impedance. Different modeling levels with their respective differential-algebraic equations are studied, to determine the minimum dynamic model of the aggregated system load that captures the most relevant features needed for voltage collapse studies of power systems. An aggregated model of a realistic load is used to illustrate the ideas presented throughout the paper.**

Keywords: bifurcations, aggregated loads, induction motor models, voltage collapse.

I. Introduction

Voltage stability problems in power systems may occur for a variety of reasons, from voltage control problems with automatic voltage regulators (AVR) and with under-load tap-changer (ULTC) transformers, to instabilities created by different types of bifurcations. Several conference proceedings and technical reports, e.g. [1, 2], summarize most of the voltage stability problems and state-of-the-art analysis techniques proposed by several researchers during the past decade, particularly those related to bifurcation theory.

Local bifurcations have been shown to cause system-wide voltage collapses and oscillatory problems in power networks [3, 4, 5, 6], leading in some cases to chaotic behavior of the corresponding mathematical model [4, 7, 8]. These bifurcations are characterized by changes in the eigenvalues of the system equilibria as certain parameters in the system change. Typically, as generation, load and/or other system parameters slowly vary, the system moves from one stable equilibrium point (s.e.p.) to another. However, for certain values of these parameters, either one system eigenvalue becomes zero (saddle-node, transcritical and pitchfork bifurcations) leading to voltage collapse problems, or a complex conjugate pair crosses the imaginary axis form left to right of the complex plane (Hopf bifurcations) generating undesirable voltage oscillations that also drive the system to voltage collapse, as demonstrated in the present paper and [9]. Although steady state models generally suffice to locate these types of bifurcations, the resulting phenomena is dynamic, leading to stability problems throughout the network. Of these bifurcations, only saddle-nodes and Hopfs are generic, i.e., they are expected to occur in the system as the parameters change, unless there is some special symmetry on the system model that leads to transcritical and/or pitchfork bifurcations [10, 11]; this particular issue is thoroughly discussed in [9] for a power system model.

Several authors have demonstrated the importance of load modeling in voltage stability studies, especially in the location of the bifurcation points and the corresponding system dynamic response [5, 6]. However, there is no general agreement in the power system community as to which particular load models are adequate for these types of study. Various reduced load models have been proposed in [12, 13, 14, 15, 16, 17] to capture the basic dynamic voltage response of the load in the system. In [18], the authors study the effect on voltage collapse of combined induction motor and impedance loads by means of lab measurements and computer simulations using some of these reduced load models. The present paper discusses a somewhat similar issue but from the point of view of bifurcation theory, using a comparable approach to the one used in [19] to study the effect on system bifurcations of different generator models. Thus, the paper focuses on discussing the effect of different models of aggregated induction motor loads, including ULTC and impedances, in system bifurcations and their corresponding effect on voltage collapse phenomena, proposing the use of a particular reduced dynamic induction machine model to adequately represent motor loads in voltage collapse studies.

Distinct methods have been proposed to successfully aggregate multiple induction motors and impedance loads. This paper uses the methodology and example proposed in [20] for aggregating impedances and induction motors, adding a basic dynamic model of a ULTC transformer to study the overall behavior of the load from the point of view of the transmission system for fifth, third and first order induction motor models.

The paper is structured as follows: In section II, the basic equations used to model a ULTC and aggregated impedances and induction motor loads are presented. The system example used throughout the paper is also introduced in this section. Section III briefly introduces some basic concepts of bifurcation theory, and relates them back to well known concepts of motor stability through the use of torque-speed characteristics. In this section, the tools and methodologies used for bifurcation analysis are presented and discussed as well. The results of applying bifurcation theory to the sample system for different motor models are analyzed in section IV, together with the effect of these models on the voltage collapse of the overall system. Based on these results, a reduced order load model is proposed in section V for adequately representing the load in voltage collapse studies.

II. System Models

A typical power system load extracted from [21] (Fig. 1) is used throughout the paper as a test system. This load is composed of 5 large induction motors of 5,600 HP (1, 3 and 4) and 1,600 HP (2 and 5), plus 5 distribution transformers and transmission lines. Each induction motor is assumed to have an additional impedance load connected at its terminals. The generator in bus 10 is used to model the power system feeding the load through an ideal ULTC, to represent a typical supply scheme.

Using the techniques described in [20], the load may be

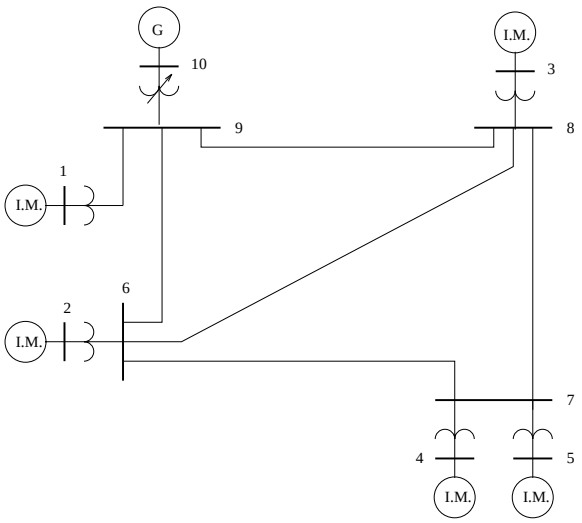

Fig. 1. Example of a realistic power system load from [21]. An equivalent generator and a ULTC have been added to the original system to represent a typical supply network.

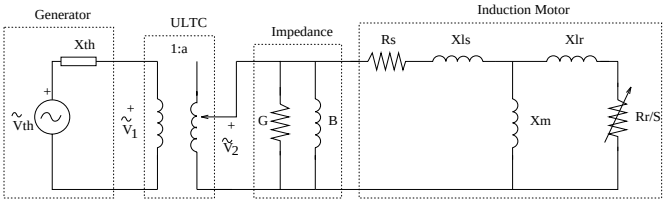

Fig. 2. Aggregated load model for the test system of Fig. 1. The generator is modeled with a simple Thevenin equivalent to represent the supply power system.

aggregated to reduced the system to the model depicted in Fig. 2, assuming a balanced three-phase system. The aggregated load is composed of a single induction motor and a static impedance load. The models used to represent the different elements of this reduced system are described below.

A. Generator

The generator was modeled with a simple Thevenin equivalent, so that one can gain insight into the load behavior without obscuring the analysis with complex generator models. (For a detailed description of the effect of different generator models in bifurcation and voltage collapse analysis review [19].) The generator is used as the system reference, i.e., $\widetilde{V}_{th} = V_{th}\angle 0^0$. Thus, the active and reactive powers P and Q delivered by the generator at the ULTC terminals can be described by the following equations, where $\widetilde{V}_1 = V_1\angle\delta_1$:

$$\begin{aligned} P &= -\frac{V_{th}V_1}{X_{th}}\sin\delta_1 \\ Q &= -\frac{V_1^2}{X_{th}} + \frac{V_{th}V_1}{X_{th}}\cos\delta_1 \end{aligned} \tag{1}$$

B. ULTC

The ULTC is assumed to be an ideal device, i.e., saturation and losses are neglected and any internal reactance is lumped into X_{th}. Therefore, the real and reactive power being injected at the ULTC from the Thevenin source is equated to the real and reactive demand of the load:

$$\begin{aligned} P &= V_2^2 G + P_{IM} \\ Q &= V_2^2 B + Q_{IM} \end{aligned} \tag{2}$$

where P_{IM} and Q_{IM} represent the powers absorbed by the equivalent machine component of the load model, and $V_2^2 G$ and $V_2^2 B$ represent the powers absorbed by the static impedance component of the load model.

To simplify the analysis of the aggregated load while retaining some of the important voltage control features of the ULTC, this paper assumes a continuous control of V_2 with no limits. However, in practice, V_2 would typically be controlled discretely by the transformer taps within certain limits. The following equations were used to model the behavior of the ideal ULTC:

$$\begin{aligned} V_2 &= aV_1 \\ \dot{a} &= \frac{1}{T_t}(V_{2_0} - V_2) \end{aligned} \tag{3}$$

where a stands for the tap shift on the secondary side with respect to a nominal 1 p.u. value, V_{2_0} is the control set point, and T_t represents the ULTC time constant. For the simulations presented in this paper, T_t is assumed to be much smaller than the typical range of 1 to 2 minutes, to better observe the system dynamic response during voltage collapse.

C. Induction Motor

The induction motor is modeled using the standard set of p.u. $dq0$ equations for a synchronously rotating reference frame connected to a balanced three-phase sinusoidal supply [22], i.e., for $\widetilde{V}_2 = V_2\angle\delta_2$,

$$\begin{aligned} v_{qs} &= \sqrt{2}\,V_2\cos\delta_2 \\ v_{ds} &= -\sqrt{2}\,V_2\sin\delta_2 \end{aligned} \tag{4}$$

$$\begin{aligned} v_{qs} &= R_s i_{qs} + \psi_{ds} + \dot{\psi}_{qs}/\omega_e \\ v_{ds} &= R_s i_{ds} - \psi_{qs} + \dot{\psi}_{ds}/\omega_e \\ 0 &= R_r i_{qr} + S\psi_{dr} + \dot{\psi}_{qr}/\omega_e \\ 0 &= R_r i_{dr} - S\psi_{qr} + \dot{\psi}_{dr}/\omega_e \end{aligned}$$

$$\begin{aligned} \psi_{qs} &= X_{ls} i_{qs} + X_m(i_{qs} + i_{qr}) \\ \psi_{ds} &= X_{ls} i_{ds} + X_m(i_{ds} + i_{dr}) \\ \psi_{qr} &= X_{lr} i_{qr} + X_m(i_{qs} + i_{qr}) \\ \psi_{dr} &= X_{lr} i_{dr} + X_m(i_{ds} + i_{dr}) \end{aligned}$$

$$\begin{aligned} T_e &= \psi_{qr} i_{dr} - \psi_{dr} i_{qr} \\ \dot{\omega}_r &= \frac{\omega_e}{2H}(T_e - T_l) \end{aligned}$$

$$\begin{aligned} P_{IM} &= 1/2\ (v_{qs} i_{qs} + v_{ds} i_{ds}) \\ Q_{IM} &= 1/2\ (v_{qs} i_{ds} - v_{ds} i_{qs}) \end{aligned}$$

Here, the machine slip $S = 1 - \omega_r/\omega_e$. The stator s and rotor r variables v, i, and ψ stand for the dq voltages, currents, and flux linkages, respectively. T_e corresponds to the electromagnetic torque generated by the machine, H represents the p.u. machine inertia, and $\omega_e = 2\pi f$ stands for the synchronous reference frame speed.

The mechanical load torque T_l is simulated as a linear function of the rotor speed as follows:

$$T_l = \frac{k}{\omega_e}\omega_r \tag{5}$$

where the constant k is used as a slow varying parameter to simulate changes in the mechanical load and, hence, in the load power demand; therefore, k represents the loading factor of the induction motor and the system. The analysis presented in this paper can be extended to any type of mechanical torque T_l, including constant and nonlinear mechanical loads.

Equations (4) are also known as the fifth order model of the induction motor (5 differential equations). Seventh order models to simulate a second rotor circuit for deep bar rotors are not discussed in this paper; however, these models can be readily reduced to fifth order models as shown in [23]. Observe that by including the stator dynamics in the motor model, the Thevenin impedance X_{th} model used to represent the feeding system is certainly insufficient to simulate the type of high frequency (above 60 Hz) dynamic phenomena typically associated with this model. Nevertheless, for the type of bifurcation (eigenvalue) analyses carried out in this paper, the authors do not believe that this would be a significant issue, since one is basically concerned with subsynchronous dynamic problems; the latter is confirmed by the results shown below for the sample system.

Reduced order models can be easily obtained from equations (4) by eliminating certain derivative terms. Thus, if the stator flux linkage transients are ignored, i.e., $\dot{\psi}_{qs} = \dot{\psi}_{ds} = 0$, the model is reduced to a third order model. Furthermore, if the rotor flux linkage transient terms are also ignored, i.e., $\dot{\psi}_{qr} = \dot{\psi}_{dr} = 0$, the model is reduced to a first order model with only one differential equation that simulates the mechanical dynamics. Finally, by eliminating all differential terms in (4), the induction motor is reduced to a simple steady state model represented by the impedances depicted in Fig. 2 with a constant slip of S. Observe that to reduce the order of the model, differential equations are basically replaced by algebraic constraints in the induction motor model.

D. Sample System Data

The aggregated load data for the system of Fig. 1 was extracted from [21], and is shown in Table I. Notice the relatively small value chosen for the ULTC time constant T_t, so that the load voltage V_2 recovers significantly faster than one would expect for typical values of T_t; nevertheless, this time constant is still much larger than the aggregated induction motor time constants, and, therefore, the overall dynamic performance does not experience qualitative changes due to this approximation. The value of the Thevenin impedance X_{th} was chosen so that "realistic" voltage values are obtained throughout the simulations.

TABLE I
AGGREGATED LOAD DATA (100MVA, 4KV BASE)

Variable	Value
R_s	0.07825
X_{ls}	0.8320
X_m	16.48
R_r	0.1055
X_{lr}	0.8320
H	0.1836 s
ω_e	$2\pi 60$ s^{-1}
G	0.06047
B	0.03530
X_{th}	0.2
T_t	5 s
V_{2_0}	1

III. BIFURCATION ANALYSIS

The scalar variable k in (5) was chosen as the "loading" or "bifurcating" parameter, as changes to this parameter have an effect on the mechanical load of the system, which result in changes to the active and reactive power demands with the corresponding effect on the load voltage; this is the typical situation encountered in voltage collapse studies. To carry this analysis, the nonlinear equations of the system were linearized at each equilibrium point for the different induction motor models. This linearized representation was then used to determine the stability of the system equilibrium points by means of eigenvalue analysis. Of particular interest are the values of k where the equilibrium points go from being stable to unstable, or from being unstable to stable, or when the number of these equilibrium points change. The operating points where these changes in stability occur are known as bifurcation points, and are typically characterized by system eigenvalues becoming zero (saddle-node, transcritical and pitchfork bifurcation), or by complex conjugate eigenvalue pairs crossing the imaginary axis (Hopf bifurcations).

The phenomena may be explained more rigorously by using the following vector representation of equations (1), (2), (3), (4) and (5):

$$\begin{aligned} \dot{x} &= f(x, y, \lambda) \\ 0 &= g(x, y, \lambda) \end{aligned} \tag{6}$$

Here, $x \in \Re^n$ is a vector of state variables, $y \in \Re^m$ is a vector of algebraic variables, and $\lambda \in \Re$ is any positive parameter in the system that changes slowly, moving the system from one s.e.p. to another until a bifurcation is encountered. The values of n and m change depending on the induction motor model used to simulate the load. For example, when the first order induction motor model is used, $n = 2$ (1 differential equation for the ULTC and 1 differential equation for the induction motor) and $m = 11$ ($n + m = 13$ in all cases). The scalar parameter λ is defined as the load torque parameter k.

For the one-parameter dynamical system (6), nonsingularity of the Jacobian $D_y g(\cdot)$ along system trajectories of interest, guarantees a well posed system [24] or strictly causal system [25, 26]. Thus, for this assumption, the following applies:

$$\begin{aligned} & y = h(x, \lambda) \\ \Rightarrow \quad & \dot{x} = f(x, h(x, \lambda), \lambda) \\ & \quad = s(x, \lambda) \end{aligned} \tag{7}$$

If $D_y g(\cdot)$ becomes singular, then the model represented by (6) breaks down. When this occurs, some algebraic constraints should be transformed into differential equations to remove the singularity by changing the system models [27], or by using singular perturbation techniques [24]. (For a detailed analysis of the dynamic behavior of systems with singular $D_y g(\cdot)$ review [28].)

A. Saddle-Node Bifurcations

Saddle-node bifurcations are characterized by two equilibrium points of (6), typically one stable (s.e.p.) and one unstable (u.e.p.), merging at the bifurcation point (x_0, y_0) for the parameter value λ_0. This equilibrium point has a simple and unique zero eigenvalue of $D_x s|_0$ in (7), which corresponds to singularities of $D_{(x,y)}F|_0$, where $F(\cdot) = [f^T(\cdot)\ g^T(\cdot)]^T$ in (6) [27]. If the two merging equilibria coexist for $\lambda < \lambda_0$, then the two equilibrium points disappear when $\lambda > \lambda_0$, or vice versa.

The saddle-node bifurcation phenomenon can be more clearly illustrated with the help of the steady state torque characteristics of the aggregated induction motor and its corresponding mechanical load in Fig. 3. A requirement of the system is that at equilibrium points the electromagnetic torque T_e and the mechanical load T_l are of equal magnitude, as expected from (4). Therefore, system equilibrium points occur at the points of intersection between the two curves in Fig. 3; the number of intersections between the two curves represent the number of equilibrium points for a given value of k. The slope of the mechanical torque varies directly with the bifurcation parameter $\lambda = k$, as governed by equation (5); therefore, as k varies, the number of intersections (equilibrium points) between the curves change in two distinct places, indicating the presence of two saddle-node bifurcations. Similar observations can be made for different mechanical loads, such as constant torque models.

The value of k for which the mechanical load T_l intersects the maximum of the electromagnetic torque T_e curve corresponds to the maximum loading point of the system. This point is typically referenced as the "knee" of the system power-voltage or PV curve. For the linear torque model used in this system, the number of crossings between the electromagnetic torque T_e and the mechanical load T_l change from 3 to 1 after this maximum loading point; hence, a saddle-node bifurcation occurs in this case on the lower half of the PV curve, "after" the knee. If a constant torque model were used, the number of crossings between the two curves would change exactly at the maximum of the electromagnetic torque, indicating that a saddle-node occurs right at the knee of the PV-curve. Similar observations have been made for a variety of load and generator models in [6, 19, 29]. The differences between maximum loading points and actual bifurcation points are clearly depicted in Figs. 5 and 7, as discussed below.

B. Hopf Bifurcations

Hopf bifurcations do not yield any changes in the number of equilibrium points. These types of bifurcations are characterized by a complex conjugate pair of eigenvalues for the equilibrium point (x_0, y_0, λ_0) of (6) lying on the imaginary axis of the complex plain. When the parameter λ changes, the complex conjugate pair moves away from the imaginary axis, either to the right or to the left of the axis. In this case, stable or unstable limit cycles (system oscillations) appear or disappear. Depending on the stability of these limit cycles and where they occur with respect to the bifurcation value parameter value λ_0, the Hopfs can be either subcritical or supercritical [10, 11].

C. Dection Methods

Direct and continuation methods can be used to detect bifurcations [11]. Direct methods have been successfully applied to determine the exact location of saddle-nodes in power systems [30, 31]; however, these methods present serious numerical difficulties when used to locate Hopf bifurcations in differential-algebraic models of the type represented by (6) [9]. Continuation methods, on the other hand, can be used in all cases to detect any type of bifurcation without major difficulties [9, 31].

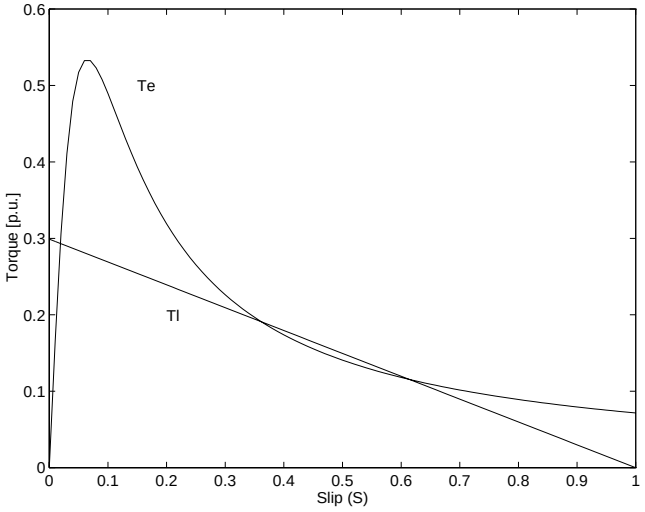

Fig. 3. Steady state torque characteristics of the aggregated induction motor and mechanical load, for $k = 0.3$. The crossing points of the electromagnetic torque T_e and the mechanical torque T_l correspond to the system equilibrium points (stable and/or unstable).

In this paper, a combination of both methods were used to determine the location and type of bifurcations in the test system. Several software packages were used to obtain the results depicted in the next section. Of these packages, AUTO94 [32] was particularly useful to determine locations and types of bifurcations, especially in the case of Hopf bifurcations where determining stability of limit cycles may be a rather difficult numerical problem [9]. Although this program was found to be an adequate tool for the work presented in this paper, it should be noted that:

1. AUTO94 required very close initial conditions to be able to converge to an initial equilibrium point; hence, other packages were used to determine good initial conditions. From the initial point, the program uses a continuation method to find other equilibrium points, and a direct method to find the bifurcation points when these are detected; AUTO94 was very robust in tracing the solution set in all directions.

2. AUTO94's output capability is initially limited to five states. A minor modification in the output code was implemented to increase this value to meet greater requirements.

3. Algebraic constraints were difficult to incorporate in AUTO94, and this became very apparent in the first and third order induction motor models. The algebraic constraints became a limiting factor in the analysis as the program assumes that the system model is made up of only differential equations. Thus, vector equations (6) were rewritten as follows:

$$\dot{x} = f(x, y, \lambda)$$

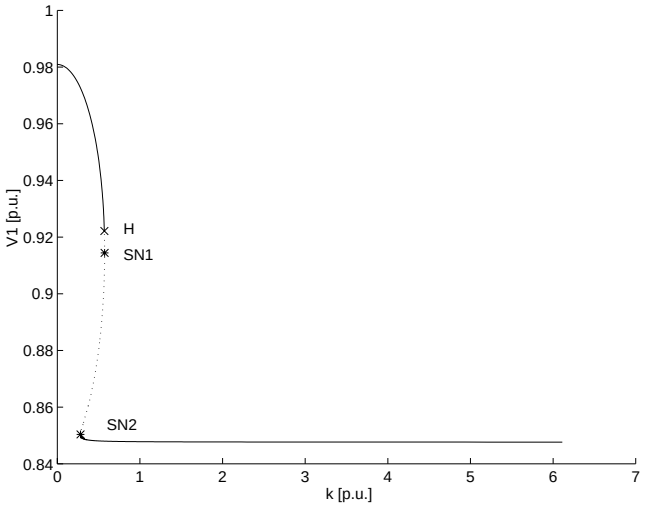

Fig. 4. Bifurcations diagram of V_1 for fifth order model. The s.e.p.s are represented with a continuos line, whereas the u.e.p.s are depicted with a dotted line.

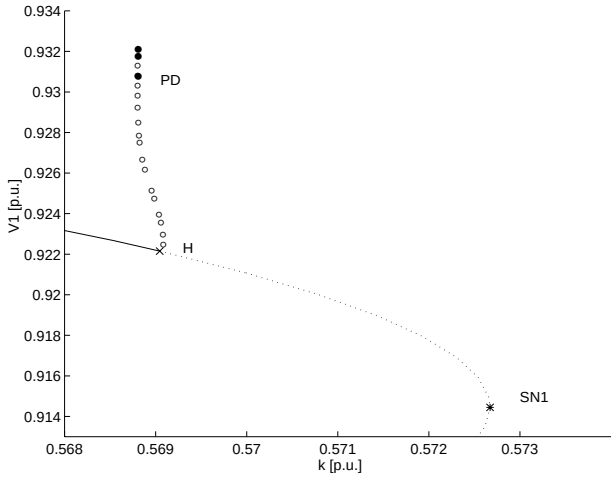

Fig. 5. Enlargement of the bifurcations diagram of Fig. 4. Stable and unstable limit cycles are depicted using black and clear circles, respectively.

$$y = h(x, \lambda)$$

so that the algebraic constraints could be directly evaluated. This required the use of other software packages to find a closed expression for the fifth order model. The closed form expressions for the first and third order models were not pursued because of their complexity; other software packages were used to study the bifurcations in these cases.

IV. Results

Equations (1), (2), (3), (4), and (5) were simulated in Auto94 in order to detect bifurcations for the test system of Fig. 2 and Table I. Using the methods described above, bifurcations diagrams for fifth, third and first order induction motor models were obtained.

Figures 4 through 7 depict the equilibrium points (stable and unstable) and bifurcations for the fifth order induction

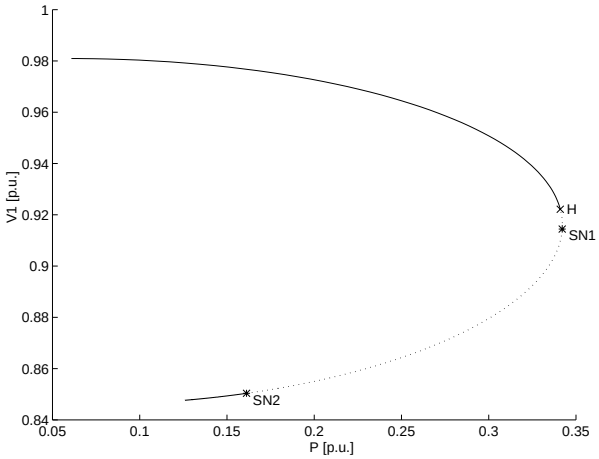

Fig. 6. PV curve of V_1 for fifth order model. The s.e.p.s are represented with a continuos line, whereas the u.e.p.s are depicted with a dotted line.

motor model, as the load varies with changes in the mechanical torque parameter k. In Fig. 4, two saddle-node bifurcations at $k_{SN_1} = 0.572672$ and $k_{SN_2} = 0.281250$ are depicted, together with a subcritical Hopf bifurcation at $k_H = 0.569044$ of an approximate period of 12.6 s. Observe that a subcritical Hopf occurs just before the first saddle-node in the loading process, which seems to be a typical phenomena in many system models [27, 9]. The limit cycles associated to the Hopf bifurcation are depicted in Fig. 4, together with a period doubling (PD) bifurcation detected along the limit cycle branch, which suggests possible chaotic behavior [4, 7, 10, 11]. The later phenomenon was not pursue any further, as better models of the transmission system and generator may be needed to better study this problem.

Figure 6 shows the total load power P versus input voltage V_1 curve for the system, i.e., the system PV curve. Observe that the Hopf bifurcation (H) occurs before the nose of the curve or maximum loading point, as clearly shown in Fig. 7. Also, this maximum loading point does not correspond exactly to the first saddle-node bifurcation (SN1), as expected from the relationship depicted in Fig. 3 between the electromagnetic torque T_e and the mechanical torque T_l; typically, these two points coincide when simplified load models are used. The second saddle-node bifurcation (SN2) indicates that stable equilibrium points exist on the lower portion of the curve; these are of no particular interest due to the rather low system voltages. (For a more detailed analysis of operation on the lower side of the PV curve for induction motors review [18].) The limit cycles and period doubling bifurcation associated to the subcritical Hopf are also depicted in the PV curve of Fig. 7.

To determine the effect of these bifurcations on the dynamic voltage response of the system, time domain simulations were carried out. In Fig. 8, the load parameter k is increased from 0.569 to 0.5691 at 2 s, to force the system to go trough the Hopf bifurcation at $k_H = 0.569044$. As expected, the voltage V_1 slowly oscillates. due to the large period of the Hopf, and then collapses, settling on an undesirable low voltage s.e.p. on the lower side of the PV curve. Similar results are obtained for the first saddle-node in all system models, although voltage oscillations are not observed in this case.

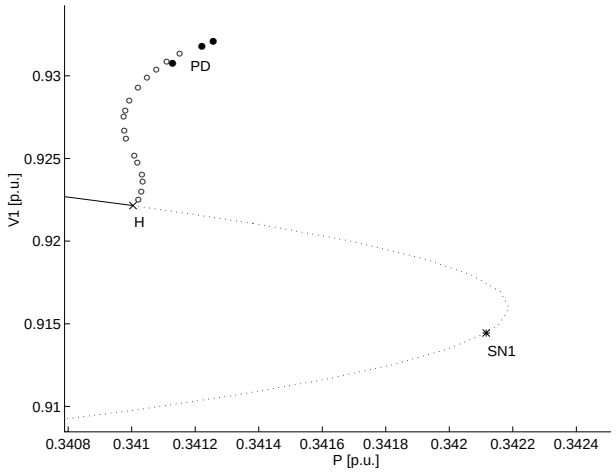

Fig. 7. Enlargement of PV curve of Fig. 4. Stable and unstable limit cycles are depicted using black and clear circles, respectively.

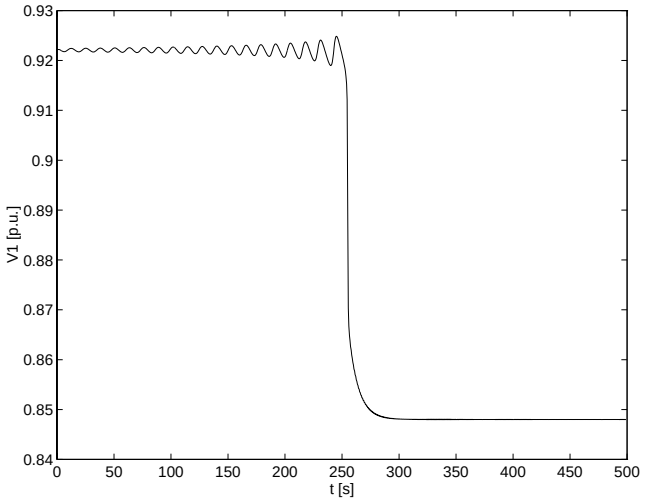

Fig. 8. Dynamic simulation of voltage V_1 collapse due to a Hopf bifurcation in the fifth order model. The value of k is changed at 2 s from 0.569 to 0.5691 ($k_H = 0.569044$).

Several tests for different system models and parameter values were also carried out to determine the effect of these models and parameters on the bifurcation points. First, for first and third order models of the induction motor, only the two saddle-node bifurcations were detected. Second, in order to determine the effect of the interaction between the induction motor and the ULTC, the model was modified so that it was composed of only an induction motor supplied from an equivalent voltage source; only the two saddle-node bifurcations were detected in this case. Finally, the values of the different impedances used to represent the static load $G + jB$ and the Thevenin impedance X_{th} were varied, observing that the presence and location of the Hopf bifurcation was a function of the value of X_{th}, and to a lesser extent, G and B. Reducing or increasing the value of X_{th} eliminates the Hopf. Thus, a Hopf bifurcation first appears for $X_{th} = 0.074$; at this point the distance between the Hopf and the first saddle-node is the greatest. This Hopf moves toward the saddle-node as X_{th} is increased, disappearing again at $X_{th} = 0.6$. Although changing G and B have similar effects on the Hopf bifurcation, larger value changes are required to obtain similar results as when changing X_{th}.

From the results shown above, one can conclude that the first order model is an acceptable approximation to the full aggregated induction motor dynamics, when the user is mostly interested in the location of saddle-node bifurcations and the dynamic behavior of the system around these points. This observation concurs with what has been shown in practice for generator models in [19, 33], i.e., higher order dynamic models are needed to study Hopf bifurcations. Steady state models are completely inadequate for bifurcation studies. Also, from the analysis of the effect of different components on the system response, one can conclude that elements in a power system cannot be evaluated independently, as their interaction may significantly affect the dynamic response.

V. Conclusions

This paper presents a complete bifurcation study of different order models of aggregated induction motors fed by ULTC transformers, and their effect on system voltage collapse. First order models of induction motors are shown to be adequate for saddle-node bifurcation studies, whereas steady state models are proven to be inadequate for these types of analyses. Thus, the paper clearly shows that at least the mechanical dynamics of aggregated loads should be included in voltage collapse studies of power systems, so that reasonable results can be obtained. When oscillatory modes associated with Hopf bifurcations are of interest, high order models must be used.

The complex dynamic behavior observed here due to the interaction of an ULTC and an aggregated induction motor load suggests that further research in bifurcation phenomena using more detailed models of the generator, static loads and transmission systems will help to understand better the interactions between the network and its different loads, possibly leading to the detection of chaotic behavior in these electrodynamical systems. For these types of studies, bifurcation analysis tools such as Auto94 will be required; however, some of the limitations of this program in handling differential-algebraic models must be resolved first. Hence, code will be developed to allow Auto94 to solve vector equations of the form presented in (6).

References

[1] L. H. Fink, editor, *Proc. Bulk Power System Voltage Phenomena III—Voltage Stability and Security*, ECC Inc., Fairfax, VA, August 1994.

[2] Y. Mansour, editor, "Suggested techniques for voltage stability analysis," technical report 93TH0620-5PWR, IEEE/PES, 1993.

[3] I. Dobson and H. D. Chiang, "Towards a theory of voltage collapse in electric power systems," *Systems & Control Letters*, vol. 13, 1989, pp. 253–262.

[4] V. Ajjarapu and B. Lee, "Bifurcation theory and its application to nonlinear dynamical phenomena in an electrical power system," *IEEE Trans. Power Systems*, vol. 7, no. 2, February 1992, pp. 424–431.

[5] J. Deuse and M. Stubbe, "Dynamic simulation of voltage collapses," *IEEE Trans. Power Systems*, vol. 8, no. 3, August 1993, pp. 894–904.

[6] C. A. Cañizares, "On bifurcations, voltage collapse and load modeling," *IEEE Trans. Power Systems*, vol. 10, no. 1, February 1995, pp. 512–522.

[7] H. D. Chiang, C. W. Liu, P. P. Varaiya, F. F. Wu, and M. G. Lauby, "Chaos in a simple power system," *IEEE Trans. Power Systems*, vol. 8, no. 4, November 1993, pp. 1407–1417.

[8] H. O. Wang, E. H. Abed, and A. M. A. Hamdan, "Bifurcation, chaos, and crises in voltage collapse of a model power system," *IEEE Tans. Circuits and Systems—I*, vol. 41, no. 3, March 1994, pp. 294–302.

[9] C. A. Cañizares and S. Hranilovic, "Transcritical and Hopf bifurcations in ac/dc systems," pp. 105–114 in [1].

[10] J. Guckenheimer and P. Holmes, *Nonlinear Oscillations, Dynamical Systems, and Bifurcations of Vector Fields*. Springer-Verlag, New York, 1986.

[11] R. Seydel, *From Equilibrium to Chaos—Practical Bifurcation and Stability Analysis*. Elsevier Science, North-Holland, 1988.

[12] K. Jimma, A. Tomac, K. Vu, and C.-C. Liu, "A study of dynamic load models for voltage collapse analysis," pp. 423–429 in [34].

[13] W. Xu and Y. Mansour, "Voltage stability analysis using generic dynamic load models," *IEEE Trans. Power Systems*, vol. 9, no. 1, 1994, pp. 479–493.

[14] D. J. Hill, "Nonlinear dynamic load models with recovery for voltage stability studies," *IEEE Trans. Power Systems*, vol. 8, no. 1, February 1993, pp. 166–176.

[15] D. Karlsson and D. J. Hill, "Modeling and identification of nonlinear dynamic loads in power systems," *IEEE Trans. Power Systems*, vol. 9, no. 1, February 1994, pp. 157–166.

[16] M. M. Begovic and R. Q. Mills, "Load identification and voltage stability monitoring," IEEE/PES 94 WM 213-9 PWRS, New York, NY, January 1994.

[17] B. C. Lesieutre, P. W. Sauer, and M. A. Pai, "Development and comparative study of induction machine based dynamic P, Q load models," IEEE/PES 94 WM 166-9 PWRS, New York, NY, January 1994.

[18] M. N. Gustafsson, N. U. Krantz, and J. E. Daalder, "Voltage stability: the significance of induction motor loads," *Proc. NAPS*, Bozeman, Montana, October 1995, pp. 394–402.

[19] P. W. Sauer, B. C. Lesieutre, and M. A. Pai, "Dynamic vs. static aspects of voltage problems," pp. 207–216 in [34].

[20] J. DiManno, G. J. Rogers, and R. T. H. Alden, "An aggregated induction motor model for industrial plants," *IEEE Trans. Power Apparatus and Systems*, vol. 103, no. 4, April 1984, pp. 683–690.

[21] T. Y. J. Lem and R. T. H. Alden, "Comparison of experimental and aggregated induction motor responses," IEEE/PES 94 WM 168-5 PWRS, New York, NY, January 1994.

[22] P. C. Krause, O. Wasynckuz, and S. D. Sudhoff, *Analysis of Electric Machinery*. IEEE Press, New York, 19995.

[23] G. Richards and P. R. R. Sarma, "Reduced order models for induction motors with two rotor circuits," IEEE/PES 94 WM 106-5 EC, New York, NY, January 1994.

[24] C. L. DeMarco and A. R. Bergen, "Application of singular perturbation techniques to power system transient stability analysis," *Proc. ISCAS*, May 1984, pp. 597–601.

[25] H. G. Kwatny, A. K. Pasrija, and L. Y. Bahar, "Static bifurcations in electric power networks: Loss of steady-state stability and voltage collapse," *IEEE Trans. Circuits and Systems*, vol. 33, no. 10, October 1986, pp. 981–991.

[26] T. Guo and R. A. Schlueter, "Identification of generic bifurcation and stability problems in power system differential-algebraic model," IEEE/PES 93 SM 513-2 PWRS, Vancouver, BC, July 1993.

[27] C. A. Cañizares, "Conditions for saddle-node bifurcations in ac/dc power systems," *Int. J. of Electric Power & Energy Systems*, vol. 17, no. 1, February 1995, pp. 61–68.

[28] V. Venkatasubramanian, H. Schättler, and J. Zaborszky, "A taxonomy of the dynamics of the large power systems with emphasis on its voltage stability," pp. 9–52 in [34].

[29] B. Lee and V. Ajjarapu, "Invariant subspace parametric sensitivity (isps) of structure-preserving power system models," IEEE/PES 95 SM 541-3 PWRS, Portland, OR, July 1995.

[30] F. L. Alvarado and T. H. Jung, "Direct detection of voltage collapse conditions," pp. 5.23–5.38 in [35].

[31] C. A. Cañizares and F. L. Alvarado, "Point of collapse and continuation methods for large ac/dc systems," *IEEE Trans. Power Systems*, vol. 8, no. 1, February 1993, pp. 1–8.

[32] E. Doedel, X. Wang, and T. Fairgrieve, "Auto94 software for continuation and bifurcation problems in ordinary differential equations," technical report, California Institute of Technology, Pasadena, CA 91125, 1994.

[33] E. H. Abed and P. P. Varaiya, "Nonlinear oscillations in power systems," *International Journal of Electric Power & Energy Systems*, vol. 6, 1984, pp. 37–43.

[34] L. H. Fink, editor, *Proc. Bulk Power System Voltage Phenomena II—Voltage Stability and Security*, ECC Inc., Fairfax, VA, August 1991.

[35] L. H. Fink, editor, *Proc. Bulk Power System Voltage Phenomena—Voltage Stability and Security*, EL-6183, EPRI, January 1989.

Claudio A. Cañizares (S'87, M'92) was born in Mexico, D.F. in 1960. In April 1984, he received the Electrical Engineer diploma from the Escuela Politécnica Nacional (EPN), Quito-Ecuador, where he was a Professor for several years. His MS (1988) and PhD (1991) degrees in Electrical Engineering are from the University of Wisconsin–Madison. Dr. Cañizares is currently an Assistant Professor at the University of Waterloo, Department of Electrical & Computer Engineering, and his research activities are mostly concentrated in the study of stability issues in ac/dc/FACTS systems.

William D. Rosehart was born in Thunder Bay, Ontario, Canada, in 1972. In May 1996, he graduated from the University of Waterloo with a Degree in Applied Science, Electrical Engineering. From 1991 to 1995 through the cooperative education program at the University of Waterloo, he worked in the Power Industry in Canada, including the Large Motors Division of GE Canada, Hammond Manufacturing, and Waterloo North Hydro. He is currently studying for his Masters degree at the University of Waterloo. His interests lie mainly in studying the effect of nonlinear loads in bifurcations of power systems.